

# The Effect of Addition Chenodeoxycholic Acid (CDCA) as Additive Material to Red Dye DN-F05 as a Color Sensitive Substance in Dye-Sensitized Solar Cell

Paramitha, Tika

Department of Chemical Engineering, Faculty of Engineering, Sebelas Maret University

Supriyanto, Agus

Department of Physics, Faculty of Mathematics and Natural Sciences, Sebelas Maret University

Widiyandari, Hendri

Department of Physics, Faculty of Mathematics and Natural Sciences, Sebelas Maret University

Nanda Yudi Shofi Subekti

Solar Cell Division, Centre of Excellence for Electrical Energy Storage Technology, Sebelas Maret University

他

<https://doi.org/10.5109/7236855>

---

出版情報 : Evergreen. 11 (3), pp.2120-2126, 2024-09. 九州大学グリーンテクノロジー研究教育センター

バージョン :

権利関係 : Creative Commons Attribution 4.0 International

# The Effect of Addition Chenodeoxycholic Acid (CDCA) as Additive Material to Red Dye DN-F05 as a Color Sensitive Substance in Dye-Sensitized Solar Cell

Tika Paramitha<sup>1,3,\*</sup>, Agus Supriyanto<sup>2,3</sup>, Hendri Widiyandari<sup>2,3</sup>,  
Nanda Yudi Shofi Subekti<sup>3</sup>, Rista Trisanti Kisdina<sup>3</sup>, Shofirul Sholikhatun Nisa<sup>3</sup>,  
Rifdha Hendianti Kisdina<sup>3</sup>, Marcus Saputra<sup>2,3</sup>, Harry Kasuma Aliwarga<sup>4</sup>

<sup>1</sup>Department of Chemical Engineering, Faculty of Engineering, Sebelas Maret University, Indonesia

<sup>2</sup>Department of Physics, Faculty of Mathematics and Natural Sciences, Sebelas Maret University, Indonesia

<sup>3</sup>Solar Cell Division, Centre of Excellence for Electrical Energy Storage Technology, Sebelas Maret University, Indonesia

<sup>4</sup>PT UMG Idealab, Indonesia

\*Author to whom correspondence should be addressed:

E-mail: tikaparamitha@staff.uns.ac.id

(Received October 30, 2023; Revised February 22, 2024; Accepted June 21, 2024).

**Abstract:** The optimization of dye in dye-sensitized solar cells (DSSCs) can improve their electrochemical performance. Therefore, this study aimed to investigate the effect of Dyenamo red dye (DN-F05) with the addition of chenodeoxycholic acid (CDCA) to inhibit the aggregation of molecules in the dye and suppress charge recombination. The results showed that the highest DSSC performance was achieved with a combination of 0.5 mM DN-F05 and 7.5 mM CDCA, with a Jsc value of 8.35 mA.cm<sup>-2</sup>, Voc 0.689 volts, and efficiency 2.988% compared to 1.974% without CDCA. Furthermore, DSSC efficiency increased slightly after 50 days, showing good stability at ambient temperature.

Keywords: dye-sensitized solar cell; chenodeoxycholic acid; DN-F05 dye; solar energy

## 1. Introduction

Currently, the problems associated with environmental pollution and a green environment are gaining significant attention. Several investigations have been carried out to developed the integration of different renewable energy into energy storage systems<sup>1</sup>). Renewable energy, sourced from nature, is abundant and inexhaustible with continuous use. In this context solar energy<sup>2-4</sup>), has shown significant potential, capable of transforming into electrical energy through the use of solar cells. The advantages of solar cells include abundant solar energy, safety, environmentally friendly, and simple installation system<sup>5</sup>). Moreover, the search for cost-effective solar cells has gained substantial attention globally, particularly Dye-Sensitized Solar Cells (DSSC)<sup>6</sup>). An ideal DSSC device consists of dye, electrolyte, counter electrode, working electrode, and transparent conductive substrate<sup>7,8</sup>). The working principle of DSSC is that when sunlight (photons) hits the photoanode, the photons will be absorbed by the dye which will then excite the electrons in the dye from the Highest Occupied Molecular

Orbital (HOMO) to the Lowest Unoccupied Molecular Orbital (LUMO). Subsequently, the semiconductor's conduction band receive the excited electrons and the dye left behind by the electrons will be in an oxidized state. The excited electrons reach the Transparent Conductive Oxide (TCO) layer and transferred to the counter electrode through an external circuit. This phenomenon leads to regeneration of oxidized dye by redox pair in the electrolyte<sup>9</sup>). The generated current depends on the distance or width of the gap between HOMO and LUMO, while the resulting voltage is based on the disparity in the redox potential level of the electrolyte and the electron Fermi level of the semiconductor<sup>10</sup>).

In DSSC, dye serves as a light sensitizer, playing a crucial role in absorbing sunlight and generating exciton. At this stage, electrons are transferred from dye LUMO to TiO<sub>2</sub> conduction band, while simultaneously injecting holes from HOMO into the redox electrolyte<sup>11</sup>). Various kinds of dye that can be used as light sensitizer include natural, metal-complex, and metal-free organic sensitizer. Several studies have been carried out regarding natural

sensitizer due to environmentally friendly properties, availability, and low production costs, but the resulting performance is still low (< 2%). Metal-complex has also shown high efficiency and stability, but requires high cost and long process for the synthesis of dye<sup>9</sup>). Metal-free organic sensitizer shows the advantages of low synthesis costs, a high extinction coefficient, environmentally friendly, and a higher absorption coefficient<sup>10</sup>). The addition of Chenodeoxycholic acid (CDCA) into dye as a co-absorbent has shown potential to increase the number of hydroxyl and carboxylic functional groups<sup>12</sup>), improving the binding of TiO<sub>2</sub> semiconductor<sup>13</sup>). This process successfully mitigates the phenomenon of dye aggregation, resulting in an enhanced electron yield<sup>14</sup>). The effects of various concentrations of CDCA on DSSC performance of the N719 dye<sup>13</sup>) were also investigated, including natural dye quercetin<sup>15</sup>) and pinang palm (*Areca catechu*) dye<sup>16</sup>).

Based on the background above, this study used metal-free organic dye with the type of 3-{6-[4-[bis(2',4'-dibutyloxybiphenyl-4-yl)amino-]phenyl]-4,4-dihexyl-cyclopenta-[2,1-b:3,4-b']dithiophene-2-yl]-2-cyanoacrylic acid (DN-F05/Dyename red, D35CPDT, LEG4), sourced from the Dyename company with the addition of various concentrations of CDCA. UV-visible (UV-Vis) and Fourier Transform Infrared (FTIR) characterizations were carried out on DN-F05 solution without and with the addition of CDCA. Subsequently, the characterization of the working electrode soaked in dye was also investigated using FTIR and Scanning Electron Microscope-Energy Dispersive X-ray (SEM-EDX). To determine the effect of adding CDCA on increasing DSSC performance, current density-voltage (J-V) characterization and cell stability were investigated. The result showed a significant improvement in DSSC performance and cell stability after 50 days, corresponding to the efficacy of CDCA supplementation.

## 2. Methodology

**Working electrode:** FTO (Fluorine-doped Tin Oxide) glass substrate (Greatcell Solar Materials) was used, measuring 2 cm × 2.5 cm, with an active area of DSSC of 0.7 cm × 0.7 cm. FTO glass was cleaned in an ultrasonic cleaner and the pre-treatment process was carried out by immersing into TiCl<sub>4</sub> (Merck) solution at 70°C for 30 min, followed by annealing at a temperature of 450°C for 45 min to block the layer<sup>17</sup>). A double layer of TiO<sub>2</sub> T-SP paste (TiO<sub>2</sub> transparent, anatase 15-20 nm, Solaronix) and TiO<sub>2</sub> R-SP paste (reflector, Solaronix) was coated on FTO glass. Subsequently, each TiO<sub>2</sub> T-SP or TiO<sub>2</sub> R-SP was coated into the substrate and heated at 450°C for 45 min using a muffle furnace. The substrate was post-treated with the same procedure as the pre-treatment process.

**Counter electrode:** FTO glass for the counter electrode was drilled to make two holes in the edge of the active area. Subsequently, cleaning was carried out using an

ultrasonic cleaner with an ethanol solution (Smartlab). Platinum paste (Solaronix) was deposited on FTO glass and the substrate was annealed at 450°C for 45 min using a muffle furnace<sup>18</sup>).

**Dye solution:** DN-F05 dye (Dyename) solution at a concentration of 0.5 mM was prepared with various CDCA (Solaronix) concentrations. Subsequently, 3 mg of DN-F05 was dissolved in 5 ml solvent of tert-butyl alcohol (Merck) and acetonitrile (Sigma Aldrich) with a volume ratio of 1:1<sup>19</sup>) by stirring at a temperature of 50°C for 2 h. CDCA variations were 5 mM, 7.5 mM, and 10 mM, as shown in Table 1.

Table 1. Sample code based on CDCA concentration.

Sample	DN-F05 (mM)	CDCA (mM)
A	0.5	0
B	0.5	5
C	0.5	7.5
D	0.5	10

**DSSC fabrication:** Working electrode substrate was immersed in 0.5 mM DN-F05 dye for 24 hours followed by rinsing using ethanol to clean dye particles that were not absorbed. Subsequently, both counter electrode and working electrode were stacked and spaced with Surlyn (Solaronix)<sup>20</sup>). Sealing process was conducted by pressing the sample using a hot press at a temperature of 250°C for 6 min. Electrolyte mosalyte TDE-250 (Solaronix) was injected into counter electrode through holes, which were sealed using silicone rubber.

**Characterization:** The four dye solutions were analyzed using UV-Vis (GENESYS 150 UV-Visible Spectrophotometer, Thermo Scientific) and FTIR (Shimadzu, Japan). UV-Vis analysis was carried out in the wavelength range of 200-800 nm and FTIR at wave numbers 400-4000 cm<sup>-1</sup>. The substrates of the working electrode were tested by SEM-EDX (JEOL, Japan) with magnifications of 5000x and 1000x and FTIR at the same wave numbers. The photovoltaic performance and impedance parameter of DSSC were characterized by the Keithley Series 2400 SourceMeter at light intensity of 1.0 sun. The characterization results in the form of short-circuit current density (J<sub>sc</sub>), open-circuit voltage (V<sub>oc</sub>), fill factor (FF), conversion efficiency, series resistance (R<sub>s</sub>), and shunt resistance (R<sub>sh</sub>) were obtained from Peccel IV Curve Analyzer 3.0 software. DSSC conversion efficiency was also determined using the equation below<sup>10</sup>):

$$\eta = \left( \frac{V_{oc} \times J_{sc} \times FF}{P_{in}} \right) \times 100\% \quad (1)$$

Where P<sub>in</sub> represents the incident power. To ensure the stability of DSSC at ambient temperature, the photovoltaic performance of the DSSC was measured after 50 days using the same procedure. The increase in efficiency after 50 days was measured using the equation below:

$$\% \text{increase in eff} = \left( \frac{\text{Eff in day 50} - \text{Eff in day 1}}{\text{Eff in day 1}} \right) \times 100\% \quad (2)$$

### 3. Result and Discussion

#### 3.1 UV-Visible Spectroscopy Characterization

The optical characteristics of DN-F05 0.5 mM without and with various CDCA concentrations were evaluated by UV-Vis irradiation. Moreover, the absorption spectra of UV-Vis are shown in Fig. 1.

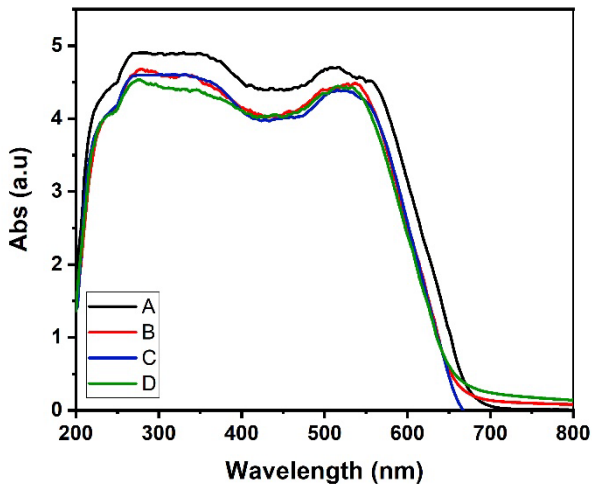


Fig 1: UV-Vis spectra of DN-F05 0.5 mM and DN-F05 0.5 mM with various CDCA concentration.

Figure 1 shows that DN-F05 0.5 mM without and with various CDCA concentrations absorb excellently in the visible region. Specifically, the results of UV-Vis irradiation of dye solution have relatively the same absorption pattern. The maximum absorption of dye in UV light was at a wavelength of 279 nm and 299 nm, while visible light was 516 nm and 536 nm. Additionally, the decrease in the absorption spectra of DN-F05 0.5 mM with various CDCA concentrations was approximately comparable. The absorption spectra of the four dye solutions gradually decreased as the concentration of CDCA increased, with the lowest absorbance obtained by adding 10 mM CDCA. A similar decrease was also observed for *A. catechu* dye due to the effect of CDCA and molecule competition<sup>16</sup>.

#### 3.2 Fourier Transform Infrared (FTIR) Characterization

DN-F05 dye solution (sample A) and DN-F05 with a CDCA concentration of 7.5 mM (sample C) were subjected to FTIR testing to determine the chemical structure, as shown in Fig. 2. Both samples, A and C, have the same functional groups, showing O-H stretching vibrations at wave number 3485 cm<sup>-1</sup>. The sharp peak at wave number 2972 cm<sup>-1</sup> indicated the C-H functional group, while C-N was observed at wave number 2253 cm<sup>-1</sup>. The presence of a band at 1366 cm<sup>-1</sup> was attributed to

the symmetric O-C-O stretch of the carboxylate (-COO-)<sup>21</sup>. Additionally, a C-O peak was found at wave number 1205 cm<sup>-1</sup>.

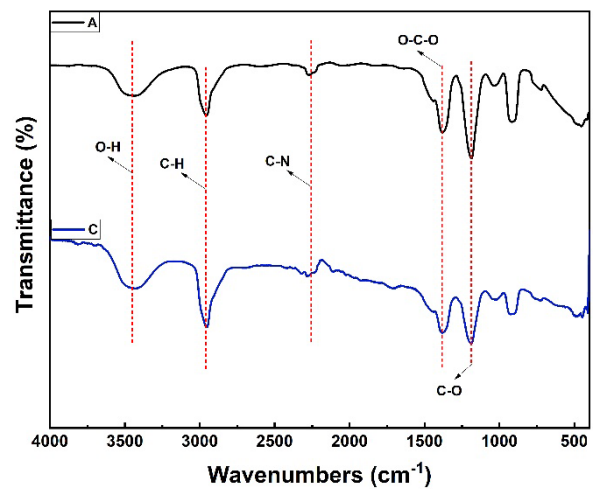


Fig 2: FTIR spectra of DN-F05 0.5 mM (sample A) and DN-F05 0.5 mM with CDCA 7.5 mM (sample C) dye solution.

Figure 3 shows FTIR spectrum of the working electrode, indicating the influence of CDCA concentration on DN-F05 0.5 mM. The interaction of the co-adsorbent molecule with dye was shown by the various functional bonds, and the vibration of each bond was observed in the transmittance spectrum.

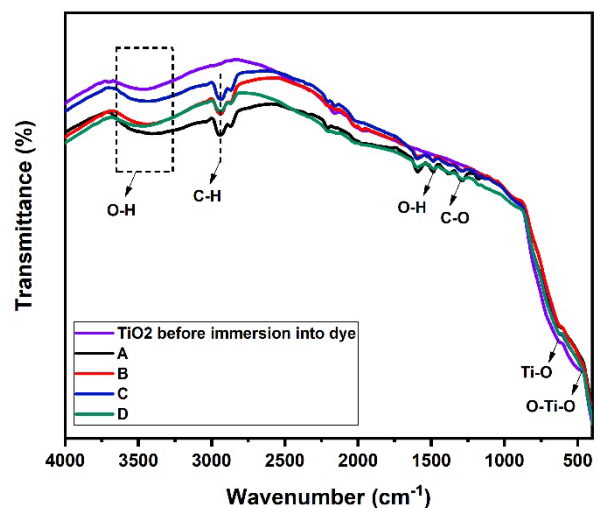


Fig 3: FTIR spectra of working electrode pure TiO<sub>2</sub> and TiO<sub>2</sub> immersed at DN-F05 0.5 mM with various concentration of CDCA.

Figure 3 shows FTIR spectra of pure and immersed TiO<sub>2</sub> at DN-F05 0.5 mM with various concentrations of CDCA. Pure TiO<sub>2</sub> has a molecular vibration band at 418 cm<sup>-1</sup>, denoting TiO<sub>2</sub> (O-Ti-O)<sup>22</sup>, along with Ti-O bond peak at 628 cm<sup>-1</sup><sup>23</sup>. Furthermore, the band appearing at 1293 cm<sup>-1</sup> was attributed to the C-O bond<sup>24</sup> and the functional group of -OH was found at approximately 1600

cm<sup>-1</sup> after immersing into DN-F05 0.5 mM with 7.5 mM CDCA. The results also showed that the presence of the band at 2932 cm<sup>-1</sup> was associated with the characteristic of C–H bond stretching<sup>25</sup>). Vibrations at a broad range of 3674 cm<sup>-1</sup> and 1172 cm<sup>-1</sup> correspond to O–H and C–O functional groups, respectively. This indicated that the addition of CDCA showed the potential to increase the level of O–H and C–O<sup>12</sup>). All dye solutions have a similar transmittance spectrum, without considering CDCA concentration, showing functional groups and vibrational bonds. The crystal lattice network on the electrode surface was observed to expand based on the strong intermolecular hydrogen bonds provided by CDCA<sup>25</sup>).

### 3.3 Current-Voltage Characterization

The performance of DSSC with various concentrations of CDCA as an additive for dye is shown in Fig. 4 and Table 2.

Table 2. Performance of DSSC sensitized with DN-F05 0.5 mM at various concentrations of CDCA.

Sample Code	Jsc (mA.cm <sup>-2</sup> )	Voc (V)	FF (%)	Eff (%)
A	6.86	0.671	42.9	1.974
B	7.36	0.671	41.2	2.035
C	8.35	0.689	51.9	2.988
D	7.92	0.663	36.1	1.897

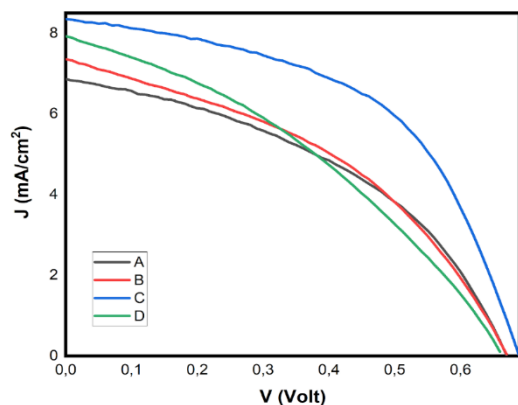


Fig 4: Current-voltage curve of DSSC sensitized with DN-F05 0.5 mM at various concentrations of CDCA.

The addition of 7.5 mM CDCA into dye DN-F05 0.5 mM shows the highest performance at 2.988% with Jsc of 8.35 mA/cm<sup>2</sup> and Voc of 0.689 volts. CDCA shows potential to inhibit the occurrence of molecular aggregation<sup>26</sup>) in dye and suppress charge recombination<sup>27</sup>), thereby increasing Jsc and Voc values.

However, DSSC performance with the addition of 10 mM CDCA into DN-F05 decreased due to different saturation levels of each solution. The addition of a higher concentration of CDCA makes dye solution more saturated, as shown by UV-Vis test in Fig. 1. A high concentration of CDCA causes a decrease in dye adsorption on TiO<sub>2</sub> substrate, leading to reduced

performance of DSSC<sup>28</sup>). In high concentrations of CDCA can replace the sensitizer<sup>26</sup>) and cause competition in the adsorption process between dye and CDCA on TiO<sub>2</sub> substrate<sup>29</sup>). This phenomenon facilitates the obstruction of TiO<sub>2</sub> surface due to high concentration of CDCA<sup>30</sup>).

Table 3. Impedance parameters of DSSC sensitized with DN-F05 0.5 mM at various concentrations of CDCA.

Sample Code	Rsh (Ω)	Rs (Ω)
A	685.299	54.162
B	421.540	62.083
C	989.381	42.081
D	396.289	69.322

FF value obtained by the device is relatively high when Rs value generated is low. This indicates an inverse relationship between Rs and FF, while Rsh and FF are directly proportional, as shown in Table 3. Rs and Rsh relationship also affects J–V curve in Fig. 4 where the crossline between A, B, and D on the middle curve occurs due to the difference of Rs. This phenomenon is attributed to the presence of a significantly large contact between the semiconductor and the electrolyte in DSSC, which increases the reduction process of I<sub>3</sub><sup>-</sup> ions in dye. Moreover, the relationship also contributes to an increase in the concentration of electrons in the semiconductor layer, which consequently reduces the amount of Rs<sup>31</sup>) and vice versa. The correlation between Rs of DSSC device and the performance can be attributed to the electron injection process from dye into the semiconductor and the charge transfer to the counter electrode. This interaction directly affects FF value, influencing the overall device performance<sup>32</sup>). Rsh corresponds to the charge recombination loss inside DSSC. Therefore, a decrease in Rs and an increase in Rsh is responsible for DSSC performance<sup>33</sup>).

### 3.4 Scanning Electron Microscope-Energy Dispersive X-ray Characterization

SEM images in Fig. 5 show TiO<sub>2</sub> layer immersed with DN-F05 0.5 mM (sample A) and DN-F05 0.5 mM with CDCA concentration of 7.5 mM (sample C). In this study, the morphology and topography of the surface of samples were determined through SEM characterization with 1000x and 5000x magnification.

As shown in Fig. 5 (b, d) the surface of the semiconductor layer without CDCA is smoother than the sample with CDCA concentration (Fig. 5 (a,c)). In comparison, the semiconductor layer with CDCA has a more porous layer. Furthermore, the large particle size of TiO<sub>2</sub> shows potential to expand the surface of TiO<sub>2</sub>. This show that there will be more photocatalytic activity to produce electron-hole pairs, thereby making self-cleaning properties more efficient<sup>34</sup>).

EDX test in Table 4 showed that the predominantly detected elements were Ti and O. Meanwhile, elements C, O and S were obtained from DN-F05 dye, while C and O

were found in CDCA. H element, which should be present in DN-F05 and CDCA, was not detected in this test.

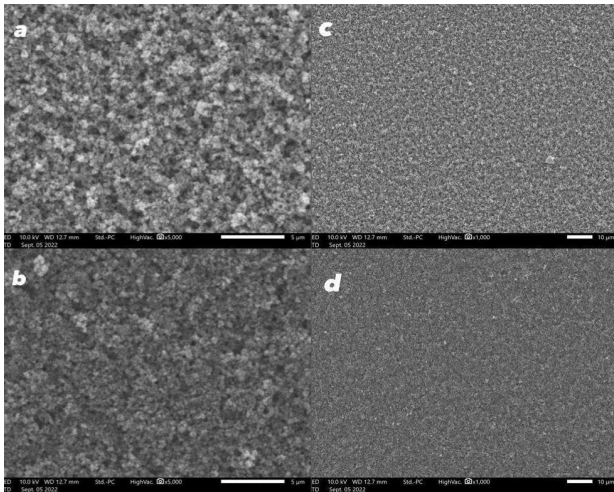


**Fig 5:** SEM images of (a,c) sample C with a magnification of 5000x and 1000x (b,d) sample A with a magnification of 5000x and 1000x.

Table 4. EDX result of Sample A and Sample C.

Element	Sample A (mass%)	Sample C (mass%)
C	0.15	0.29
O	38.50	40.71
S	0.12	0.16
Ti	61.23	58.85

### 3.5 Stability Performance

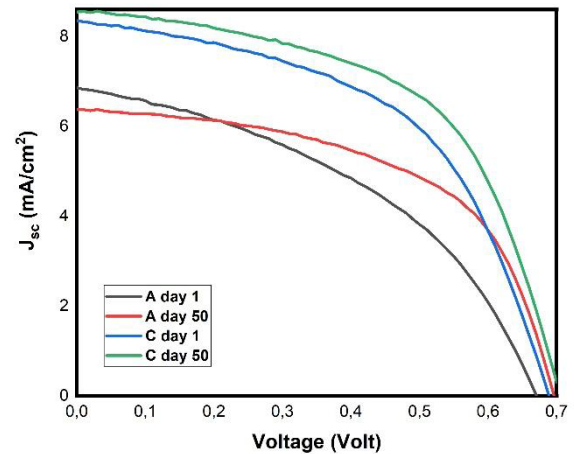
The sample was sealed using surlyn and silicone glue as the primary and hole sealing materials, respectively. The main function of the sealing materials in DSSC is to prevent any leaking of electrolytes toward the cells<sup>35</sup>. To further confirm the stability of DSSC under ambient temperature, the photovoltaic performance of DSSC was measured after 50 days, as shown in Table 4 and Fig. 6. The measurement results presented in Table 5 show an increase in voltage and current, with a slight improvement in DSSC efficiency between 12.3%-24.3% from day 1, indicating good stability at ambient temperature.

Table 5. Stability performance of DSSC sensitized with DN-F05 0.5 mM at various concentrations of CDCA.

Sample	Days	Jsc (mA.cm <sup>-2</sup> )	Voc (V)	FF (%)	Eff (%)
A	1	6.86	0.671	42.9	1.974
	50	6.37	0.696	55.3	2.455
C	1	8.35	0.689	51.9	2.988
	50	8.55	0.705	55.7	3.357

Figure 6 shows that there are crossed lines in sample A but not in sample C on day 1 and day 50. This difference is attributed to a significant increase in the value of Rsh and a decrease in Rs in sample A. The combination of Rsh and Rs values will produce a current-voltage (J-V) curve that reaches a rectangular shape<sup>36</sup>. Meanwhile, in sample

C, there is no significant increase in Rsh or decrease in Rs, showing a similar trend in J-V curve as shown in Table 6.



**Fig 6:** Current-voltage stability curve of samples A and C.

Table 6. DSSC impedance parameters on day 1 and day 50.

Sample	Day	Rsh (Ω)	Rs (Ω)
A	1	685.299	54.162
	50	1800.164	35.644
C	1	989.381	42.081
	50	1591.288	35.806

## 4. Conclusion

In conclusion, this study successfully investigated the effect of adding CDCA to DN-F05 dye. The optical properties, functional groups, surface morphology, composition, and photovoltaic performance of all DSSC samples have been studied. The results of UV-vis analysis showed that the addition of CDCA could reduce the absorption spectra of dye solution. DN-F05 dye solution without and with CDCA had the same functional groups. FTIR characterization showed a significant increase in the absorption spectrum of the -OH and C-O functional groups, along with DSSC performance at ambient temperature. The optimum addition of CDCA was obtained at 0.5 mM DN-F05 with a concentration of 7.5 mM, which showed Jsc value of 8.35 mA, Voc of 0.689 volts, and efficiency of 2.988%. Similarly, SEM results showed that the addition of CDCA had more pores facilitating increased dye absorption and higher photovoltaic performance. Based on EDX analysis, the predominant elements were found to be Ti and O. After 50 days, DSSC efficiency increased by 12.3%-24.3% from day 1, showing good stability at ambient temperature.

## Acknowledgements

The authors are grateful to the PT UMG Idealab and Matching Fund Program 2022 (Contract No.: 017/PKS/UMGIDEA-UNS/LEG/VII/2022 and 119/UN27/KS/2022) for financial sponsorship.

## Nomenclature

$\eta$	power conversion efficiency (%)
$P_{in}$	incident light intensity
$FF$	fill factor (%)
$J_{sc}$	short-circuit photocurrent density ( $mA/cm^2$ )
$V_{oc}$	open-circuit photovoltage (Volt)

## References

- M. Duan, Y. Rong, A. Mei, Y. Hu, Y. Sheng, Y. Guan, and H. Han, "Efficient hole-conductor-free, fully printable mesoscopic perovskite solar cells with carbon electrode based on ultrathin graphite," *Carbon N. Y.*, **120**, 71–76 (2017). doi:10.1016/j.carbon.2017.05.027.
- S.K.S. R. Kumar, S. K. Verma, N. K. Gupta, "Performance enhancement of tsah using graphene and graphene / ceo 2 -black paint coating on absorber : a comparative study," *Evergreen*, **09** (03) 673–681 (2022). doi:https://doi.org/10.5109/4843098.
- K. Marzia, M.F. Hasan, T. Miyazaki, B.B. Saha, and S. Koyama, "Key factors of solar energy progress in bangladesh until 2017," *Evergreen*, **5** (2) 78–85 (2018). doi:10.5109/1936220.
- T. Hanada, "Modifying the feed-in tariff system in japan: an environmental perspective," *Evergreen*, **3** (2) 54–58 (2016). doi:10.5109/1800872.
- T.V.S.S.P. Sashank, B. Manikanta, and A. Pasula, "Fabrication and experimental investigation on dye sensitized solar cells using titanium dioxide nano particles," *Mater. Today Proc.*, **4** (2) 3918–3925 (2017). doi:10.1016/j.matpr.2017.02.291.
- N. Akter, A. Hossion, and N. Amin, "Fabrication of oxide passivated and antireflective thin film coated emitter layer in two steps for the application in photovoltaic," *Evergreen*, **9** (3) 654–661 (2022). doi:10.5109/4842524.
- A.A.F. Husain, W.Z.W. Hasan, S. Shafie, M.N. Hamidon, and S.S. Pandey, "A review of transparent solar photovoltaic technologies," *Renew. Sustain. Energy Rev.*, **94** (January 2017) 779–791 (2018). doi:10.1016/j.rser.2018.06.031.
- Z. Arifin, S. Hadi, Suyitno, B. Sutanto, and D. Widhiyanuriyawan, "Investigation of curcumin and chlorophyll as mixed natural dyes to improve the performance of dye-sensitized solar cells," *Evergreen*, **9** (1) 17–22 (2022). doi:10.5109/4774212.
- N.T.R.N. Kumara, A. Lim, C.M. Lim, M.I. Petra, and P. Ekanayake, "Recent progress and utilization of natural pigments in dye sensitized solar cells: a review," *Renew. Sustain. Energy Rev.*, **78** (July 2016) 301–317 (2017). doi:10.1016/j.rser.2017.04.075.
- M.A.M. Al-Alwani, A.B. Mohamad, N.A. Ludin, A.A.H. Kadhum, and K. Sopian, "Dye-sensitised solar cells: development, structure, operation principles, electron kinetics, characterisation, synthesis materials and natural photosensitisers," *Renew. Sustain. Energy Rev.*, **65** 183–213 (2016). doi:10.1016/j.rser.2016.06.045.
- D. Kishore Kumar, J. Křiž, N. Bennett, B. Chen, H. Upadhayaya, K.R. Reddy, and V. Sadhu, "Functionalized metal oxide nanoparticles for efficient dye-sensitized solar cells (dsscs): a review," *Mater. Sci. Energy Technol.*, **3** 472–481 (2020). doi:10.1016/j.mset.2020.03.003.
- M. Ismail, N. Ahmad Ludin, N. Hisham Hamid, M. Adib Ibrahim, and K. Sopian, "The effect of chenodeoxycholic acid (cdca) in mangosteen (garcinia mangostana) pericarps sensitizer for dye-sensitized solar cell (dssc)," *J. Phys. Conf. Ser.*, **1083** (1) (2018). doi:10.1088/1742-6596/1083/1/012018.
- H. Trilaksana, C. Shearer, L. Kloo, and G.G. Andersson, "Restructuring of dye layers in dye sensitized solar cells: cooperative adsorption of n719 and chenodeoxycholic acid on titania," *ACS Appl. Energy Mater.*, **2** (1) 124–130 (2019). doi:10.1021/acsaem.8b01864.
- J. Zhang, A. Zhong, G. Huang, M. Yang, D. Li, M. Teng, and D. Han, "Enhanced efficiency with cdca co-adsorption for dye-sensitized solar cells based on metallosalophen complexes," *Sol. Energy*, **209** (September) 316–324 (2020). doi:10.1016/j.solener.2020.08.096.
- G. Chayal, K. Ram, M. Saran, M. Kumar, N. Prasad, and K. Shitiz, "Effect of surface treatment on photovoltaic properties of dye-sensitized solar cell based on natural dye quercetin," **96** (August) 1059–1065 (2019).
- A.S. Najm, N.A. Ludin, N.H. Hamid, M.A. Ibrahim, M.A.M. Teridi, K. Sopian, H. Moria, A.M. Holi, A.A. Al-Zahrani, and H.S. Naeem, "Effect of chenodeoxycholic acid on the performance of dye-sensitized solar cells utilizing pinang palm (areca catechu) dye," *Sains Malaysiana*, **49** (12) 3017–3028 (2020). doi:10.17576/jism-2020-4912-13.
- T. Paramitha, D.A. Munika, D.R. Saputra, S.S. Nisa, A. Purwanto, A. Supriyanto, H. Widiyandari, and H.K. (Kiwi) Aliwarga, "Application of rice husk as a carbon source for substitution of sensitizer and counter electrode material in dye-sensitized solar cells," *J. Phys. Conf. Ser.*, **2696** (012010) (2024). doi:10.1088/1742-6596/2696/1/012010.
- T. Paramitha, R. Rafela, M.H. Zahro, and S.S. Nisa, "Fabrication of tio 2 -ag composites for working electrode of dye-sensitized solar cells," *E3S Web Conf.*, **01005** (481) 1–9 (2024).
- W. Yang, N. Vlachopoulos, Y. Hao, A. Hagfeldt, and G. Boschloo, "Efficient dye regeneration at low driving force achieved in triphenylamine dye leg4 and tempo redox mediator based dye-sensitized solar cells," *Phys. Chem. Chem. Phys.*, **17** (24) 15868–

- 15875 (2015). doi:10.1039/c5cp01880c.
- 20) S. Rahayu, A.T. Dosi, and P. Wulandari, "Optimization of metal nanoparticles concentration in dye solution to enhance performance of dye sensitized solar cells," *J. Phys. Conf. Ser.*, **2243** (1) (2022). doi:10.1088/1742-6596/2243/1/012090.
- 21) V. Leandri, W. Yang, J.M. Gardner, G. Boschloo, and S. Ott, "Rapid microwave-assisted self-assembly of a carboxylic-acid-terminated dye on a tio2 photoanode," *ACS Appl. Energy Mater.*, **1** (1) 202–210 (2018). doi:10.1021/acsaem.7b00088.
- 22) S.B. Wategaonkar, R.P. Pawar, V.G. Parale, D.P. Nade, B.M. Sargar, and R.K. Mane, "Synthesis of rutile tio2 nanostructures by single step hydrothermal route and its characterization," *Mater. Today Proc.*, **23** 444–451 (2020).
- 23) F. Saadmim, T. Forhad, A. Sikder, W. Ghann, M.M. Ali, V. Sitther, A.J.S. Ahammad, M.A. Subhan, and J. Uddin, "Enhancing the performance of dye sensitized solar cells using silver nanoparticles modified photoanode," *Molecules*, **25** (17) (2020). doi:10.3390/molecules25174021.
- 24) A. Ricci, K.J. Olejar, G.P. Parpinello, P.A. Kilmartin, and A. Versari, "Application of fourier transform infrared (ftir) spectroscopy in the characterization of tannins," *Appl. Spectrosc. Rev.*, **50** (5) 407–442 (2015). doi:10.1080/05704928.2014.1000461.
- 25) A.S. Najm, N.A. Ludin, M.F. Abdullah, M.A. Almessiere, N.M. Ahmed, and M.A.M. Al-Alwani, "Areca catechu extracted natural new sensitizer for dye-sensitized solar cell: performance evaluation," *J. Mater. Sci. Mater. Electron.*, **31** (4) 3564–3575 (2020). doi:10.1007/s10854-020-02905-x.
- 26) A. Dhar, N. Siva Kumar, M. Asif, and R.L. Vekariya, "Fabrication of d- $\pi$ -a sensitizers based on different donors substituted with a dihydropyrrolo[3,4-c]pyrrole-1,4-dione bridge for dsscs: influence of the cdca co-absorbent," *New J. Chem.*, **42** (14) 12024–12031 (2018). doi:10.1039/c8nj00847g.
- 27) Z. Wang, X.F. Zang, H. Shen, C. Shen, X. Ye, Q. Li, Y.Y. Quan, F. Ye, and Z.S. Huang, "Dithienopyrrolobenzothiadiazole-based metal-free organic dyes with double anchors and thiophene spacers for efficient dye-sensitized solar cells," *Sol. Energy*, **208** (September) 1103–1113 (2020). doi:10.1016/j.solener.2020.08.064.
- 28) A.S. Najm, N. Ahmad Ludin, I. Jaber, N.H. Hamid, and H. Salah Naeem, "Influence of the concentration of chenodeoxycholic acid on the performance of the n719 dye," *Inorganica Chim. Acta*, **533** (November 2021) (2022). doi:10.1016/j.ica.2021.120776.
- 29) A.F. Buene, D.M. Almenningen, A. Hagfeldt, O.R. Gautun, and B.H. Hoff, "First report of chenodeoxycholic acid-substituted dyes improving the dye monolayer quality in dye-sensitized solar cells," *Sol. RRL*, **4** (4) (2020). doi:10.1002/solr.201900569.
- 30) L. Favereau, Y. Pellegrin, L. Hirsch, A. Renaud, A. Planchat, E. Blart, G. Louarn, L. Cario, S. Jobic, and M. Boujtita, "Engineering processes at the interface of p-semiconductor for enhancing the open circuit voltage in p-type dye-sensitized solar cells," **7** (12) 1601776 (2017). doi:10.1002/aenm.201601776i.
- 31) A. Agrawal, S.A. Siddiqui, A. Soni, K. Khandelwal, and G.D. Sharma, "Performance analysis of tio2 based dye sensitized solar cell prepared by screen printing and doctor blade deposition techniques," *Sol. Energy*, **226** (August) 9–19 (2021). doi:10.1016/j.solener.2021.08.001.
- 32) N. Kutlu, "Investigation of electrical values of low-efficiency dye-sensitized solar cells (dsscs)," *Energy*, **199** 117222 (2020). doi:10.1016/j.energy.2020.117222.
- 33) R. Chen, Y. Feng, L. Jing, M. Wang, H. Ma, J. Bian, and Y. Shi, "Low-temperature sprayed carbon electrode in modular htl-free perovskite solar cells: a comparative study on the choice of carbon sources," *J. Mater. Chem. C*, **9** (10) 3546–3554 (2021). doi:10.1039/d0tc05528j.
- 34) A. Azani, D.S.C. Halin, M.M. Al Bakri Abdullah, K.A. Razak, M.F.S.A. Razak, M.M. din Ramli, M.A.A.M. Salleh, and V. Chobpattana, "The effect of go/tio2 thin film during photodegradation of methylene blue dye," *Evergreen*, **8** (3) 556–564 (2021). doi:10.5109/4491643.
- 35) N.M. Nursam, J. Hidayat, L. Muliani, P.N. Anggraeni, L. Retnaningsih, and N. Idayanti, "From cell to module: fabrication and long-term stability of dye-sensitized solar cells," *IOP Conf. Ser. Mater. Sci. Eng.*, **214** (1) (2017). doi:10.1088/1757-899X/214/1/012007.
- 36) M. Diantoro, T. Suprayogi, A. Hidayat, A. Taufiq, A. Fuad, and R. Suryana, "Shockley's equation fit analyses for solar cell parameters from i-v curves," *Int. J. Photoenergy*, **2018** (2018). doi:10.1155/2018/9214820.